An Effectiveness--Number of Transfer Units Relationship for Evaporators With Non-negligible Boiling Point Elevation Increases

Citation: Thiel, Gregory P., and John H. Lienhard. "An Effectiveness–Number of Transfer Units Relationship for Evaporators With Non-Negligible Boiling Point Elevation Increases." Journal of Heat Transfer 138, no. 12 (August 2, 2016): 121801. © 2016 ASME.

As Published: http://dx.doi.org/10.1115/1.4034055

Publisher: American Society of Mechanical Engineers (ASME)

Persistent URL: http://hdl.handle.net/1721.1/105437

Version: Final published version: final published article, as it appeared in a journal, conference proceedings, or other formally published context

G.P. Thiel and J.H. Lienhard V, "An effectiveness-NTU relationship for evaporators with non-negligible boiling point elevation increases," Journal of Heat Transfer, 138(12):12180, December 2016.

An effectiveness–NTU relationship for evaporators with non-negligible boiling point elevation increases

Gregory P. Thiel

Postdoctoral Associate, Member of ASME
Rohsenow Kendall Heat and Mass Transfer Laboratory
Department of Mechanical Engineering
Massachusetts Institute of Technology
Cambridge, MA 02139 USA
Email: gpthiel@alum.mit.edu

John H. Lienhard V

Professor, Fellow of ASME
Rohsenow Kendall Heat and Mass Transfer Laboratory
Department of Mechanical Engineering
Massachusetts Institute of Technology
Cambridge, MA 02139 USA
Email: lienhard@mit.edu

An effectiveness number of transfer units (ε-NTU) model is developed for use in evaporators where the evaporating stream: (1) comprises a volatile solvent and non-volatile solute(s); and (2) undergoes a significant, but linear change in boiling point elevation with increasing solute molality. The model is applicable to evaporators driven by an isothermal stream (e.g., steam-driven or refrigerant-driven) in parallel flow, counterflow, and crossflow configurations where the evaporating stream is mixed. The model is of use in a variety of process engineering applications as well as the sizing and rating of evaporators in high-salinity desalination systems.

Nomenclature

Roman Symbols

A Area, m^2
B_i Constants in Eq. (47) defined by Eqs. (48)–(52)
b Molality, mol/kg
C_i Constants defined by Eqs. (40)–(44)
c_p Specific heat capacity, $\partial h/\partial T|_{P,\omega}$, J/kg K
$\mathscr{D}$ Diffusivity, m^2/s
D_0 Constant in Eq. (36), $[3\mu\Gamma/\rho g(\rho-\rho_v)]^{1/3}$
h Solution enthalpy, J/kg-solvent
h_A Solvent enthalpy, J/kg
h_B Apparent enthalpy of the solute, J/kg-solvent
h_v Vapor enthalpy, J/kg
h_{conv} Convective heat transfer coefficient
h_{fg} Enthalpy of vaporization, J/kg
j' Mass transfer rate per unit length, kg/m
$\overline{K}_b$ Modified ebullioscopic constant, K
L Length, m
M Molar mass, kg/mol
$\dot{m}$ Mass flow rate, kg/s
$\mathscr{P}$ Heat transfer area per unit length, A/L, m
q' Heat transfer rate per unit length, W/m
R Universal gas constant, J/mol K
T Temperature
ΔT_{bp} Boiling point elevation, K
U Overall heat transfer coefficient, W/m^2-K
w Solute mass fraction

Greek Symbols

Γ Film flow rate per unit width, kg/m s
γ Dimensionless parameter, θ_0/θ_H
ε Effectiveness
θ Temperature difference, $T - T_s^\circ$
ϕ Molal osmotic coefficient
μ Dynamic viscosity, kg/m s
ν Solute stoichiometric coefficient
ρ Density, kg/m^3
χ Evaporated fraction
ω Solute mass ratio

Dimensionless Numbers

CF Concentration factor, w_L/w_0
$\mathrm{CF}_{\max}$ Maximum concentration factor, w_H/w_0
Ja Jakob number, $c_p\Delta T/h_{fg}$
NTU Number of transfer units, $UA/\dot{m}_{A0}c_p$
Nu Nusselt number, $h_{\mathrm{conv}}L/k$
Pr Prandtl number, $\mu c_p/k$
Re Reynolds number, $4\Gamma/\mu$
Sc Schmidt number, $\mu/\rho\mathscr{D}$

Subscripts

0 Inlet state
A Solvent
B Solute
δ Liquid-vapor interface
H Hot stream
L Outlet state
s Saturated state
v Vapor
w Wall

Superscripts

$\circ$ Reference (pure solvent) state

1 Introduction

Falling film evaporators are used in a variety of applications, including desalination, refrigeration, solvent recovery, juice concentration, and many others [1, 2]. The transport phenomena in falling films—both evaporation and condensation, which have significant overlap—have been widely studied since Nusselt's now classical analysis [3]. Many effects not included in Nusselt's initial analysis, including vapor shear [4], turbulence [5–8], nucleate boiling [9, 10], critical heat flux [11], the hydrodynamics of films falling over tubes [12–15], and tube enhancement [16–18] have been experimentally and theoretically investigated and reviewed [19–21] extensively.

In some evaporators, such as those used in the desalination of high-salinity waters, the rise in temperature of the evaporating stream owing to boiling point elevation increase may be nonneglible [22, 23]. In such cases, neither classical effectiveness–NTU relationships [24], which are valid for constant capacity rates, nor traditional falling film evaporation analysis [25, 26], which generally considers uniform vapor saturation temperature, are applicable. Existing studies on falling film evaporation for brines [27, 28] are generally restricted to concentrations well below NaCl saturation, which is of practical interest in high-salinity desalination systems. In this work, we develop an alternative relationship for cases where the boiling point elevation is a linear function of the non-volatile solute concentration. The work provides an analytical framework for sizing and rating evaporators in many applications.

2 Modeling Approximations

In developing the ε-NTU relationship, we make the following modeling approximations, each of which will be discussed in detail:

1. The mixture enthalpy is the sum of a pure solvent enthalpy and the apparent enthalpy of the non-volatile solute(s), written per unit solvent
2. The bulk state of the evaporating liquid is treated as saturated at the local composition
3. The boiling point elevation varies linearly with the molality of the solute
4. The heat transfer in the vapor phase is neglected

2.1 Mixture Enthalpy

In order to simplify the mathematical treatment, we write the enthalpy of the solution in a form that mimics moist air mixtures:

$$h = h_A + \omega h_B \tag{1}$$

where h is the solution enthalpy per unit mass of solvent, h_A is the enthalpy of the pure solvent (e.g., water), h_B is the apparent enthalpy of the solute(s) [29], and ω is the ratio of solute mass to solvent mass. So written, h_A is only a function of temperature; the concentration dependence of the solution enthalpy is contained entirely within h_B. The mass ratio of solute to solvent, $\omega = bM_B$, where b is the solute molality and M_B is the molar mass of the solute.

2.2 Bulk Saturation

In falling film evaporation, the liquid at the vapor–liquid interface is at the saturation temperature corresponding to the pressure and local solute concentration. In this model, we approximate the bulk solute concentration as equal to the concentration at the vapor–liquid interface, which introduces little error, as shown by the integral method analysis of the mass transfer boundary layer by Chun and Seban [27]. For a parabolic concentration profile with zero solute flux at the vapor–liquid interface, a zero concentration gradient at the wall, and a wall concentration specified by solute mass conservation, Chun and Seban showed that the ratio of the solute mass fraction at the vapor–liquid interface, w_δ, to the average value, w, is

$$\frac{w_\delta}{w} = \left[1 - \frac{1}{5}\frac{\mathrm{Sc\,Ja}}{\mathrm{Pr}}\right]^{-1} \tag{2}$$

which, for typical values of Sc, Ja, and Pr (e.g., for NaCl solutions), is between 1 and 1.05.

2.3 BPE Linearity

Figure 1 shows that the boiling point elevation (BPE), ΔT_{bp}, has a nearly linear dependence on ω for several common solutes in water over a wide range of concentrations.

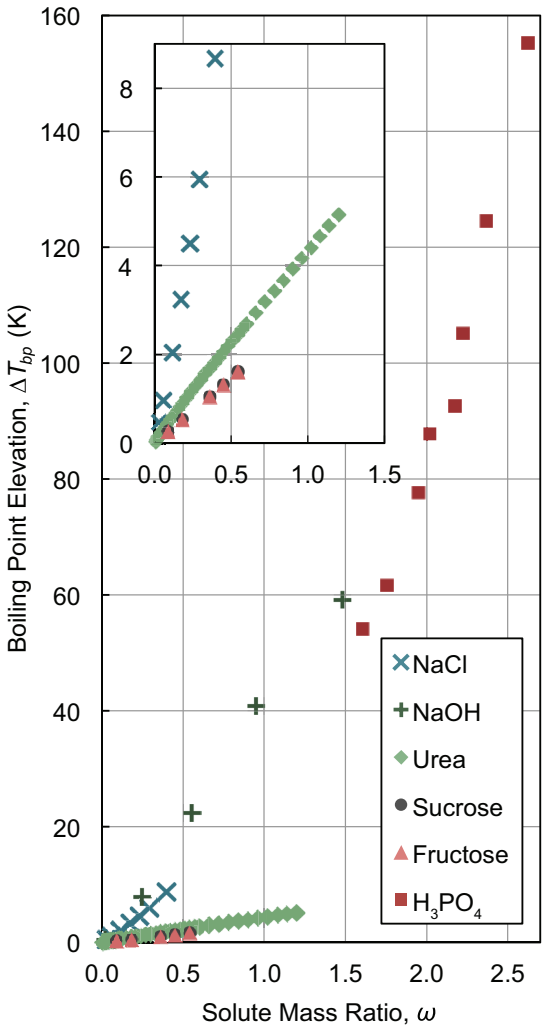

Fig. 1: The boiling point elevation for some common aqueous mixtures is linear over a wide range of concentrations; the data are adapted from [30–32] and are at atmospheric pressure except for urea, which is at 3.17 kPa.

We thus linearize this dependence, as

$$\Delta T_{bp} = T_s - T_s^\circ = \overline{K}_b \omega \tag{3}$$

where T_s° is the saturation temperature of the pure solvent at the given pressure, and $\overline{K}_b$ is a modified ebullioscopic constant (cf. [29]):

$$\overline{K}_b = \frac{\nu R T_s^{\circ 2} \phi}{M_B h_{fg}^\circ} \tag{4}$$

where ν is the solute stoichiometric coefficient (i.e., the number of solute molecules in the aqueous phase per molecule dissolved solid; $\nu = 2$ for NaCl); h_{fg}° is the enthalpy of vaporization for the pure solvent; ϕ is the osmotic coefficient, evaluated at the highest concentration of interest; and R is the universal gas constant. Such a linearization overpredicts the BPE of NaCl solutions by no more than 0.47 K when the curve is linearized from zero to saturation salinities. When linearized over a smaller salinity range, as would be typical, e.g., for many desalination systems, the associated error decreases.

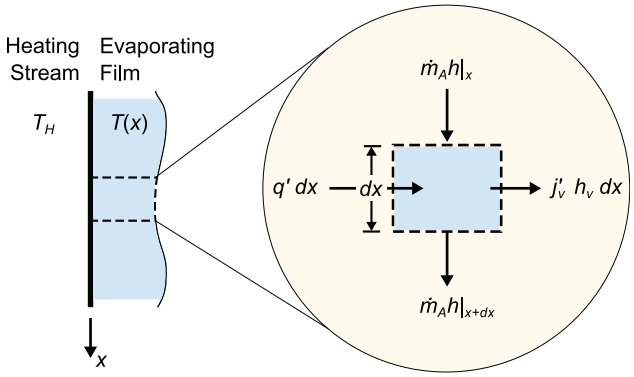

Fig. 2: Differential control volume of an evaporating stream: the solution enters at position x, pure solvent is vaporized at a rate $j_v' dx$, and the concentrated solution leaves the control volume at position $x + dx$. The evaporation is driven by a heat transfer rate $q' dx$.

2.4 Vapor-Phase Heat Transfer

Because the vapor–liquid interface temperature increases along the streamwise coordinate, the evaporated vapor is not in thermal equilibrium, as is the case for typical falling-film analyses [25, 26]. Depending on the extent of evaporation, the vapor at the evaporator outlet may be several degrees warmer than at the inlet. Nevertheless, for stagnant or near-stagnant vapor, the energy associated with any heat transfer in the vapor phase is small compared to the energy associated with the phase transformation at the vapor–liquid interface. We thus neglect any heat transfer in the vapor phase, and base the heat transfer process on the temperature difference across the hot stream and the evaporating film, as is typical in falling-film analysis.

3 Model Development

To develop the effectiveness-NTU relation, we solve an ODE derived from energy, mass, and solute conservation applied to a differential control volume of the evaporating stream. Consider such a differential control volume, as shown in Fig. 2: a feed solution enters at x, pure solvent evaporates at a rate $\delta\dot{m} = j_v' dx$, and the concentrated solution stream leaves at position $x + dx$. A heat transfer rate $q' dx$ from an isothermal stream (e.g., condensing steam or refrigerant) at T_H drives the evaporation.

Conservation of energy on this control volume requires that

$$\frac{d(\dot{m}_A h)}{dx} = q' - j_v' h_v \tag{5}$$

where $\dot{m}_A$ is the mass flow rate of pure solvent, h is the solution (mixture) enthalpy, written *per unit solvent*, q' is the heat transfer rate per unit length, j'_v is the mass flux of vapor (per unit length), and h_v is the enthalpy of pure vapor. Expanding the derivative yields

$$\dot{m}_A \frac{dh}{dx} + h\frac{d\dot{m}_A}{dx} = q' - j'_v h_v \tag{6}$$

As the dissolved solutes do not evaporate, $d(\dot{m}_A \omega) = 0$, so:

$$j'_v = \frac{d\dot{m}_A}{dx} = -\frac{\dot{m}_A}{\omega}\frac{d\omega}{dx} \tag{7}$$

Thus, Eq. (6) can be rewritten

$$\dot{m}_A \left[\left.\frac{\partial h}{\partial T}\right|_\omega \frac{dT}{dx} + \left(\left.\frac{\partial h}{\partial \omega}\right|_T + \frac{h_v - h}{\omega} \right) \frac{d\omega}{dx} \right] = q' \tag{8}$$

Approximating the bulk state of the evaporating stream as a saturated, isobaric liquid, we write T as the saturation temperature at a particular solute mass ratio ω. Substituting Eq. (1) and (7) into Eq. (8) and simplifying, we find

$$\dot{m}_A \frac{dT}{dx} \left[c_p + \left(\omega \left.\frac{\partial h_B}{\partial \omega}\right|_T + \frac{h^\circ_{fg}}{\omega} \right) \frac{d\omega}{dT} \right] = q' \tag{9}$$

where the specific heat capacity $c_p = \partial h/\partial T|_{P,\omega}$. In order to separate and integrate Eq. (9), we require $\dot{m}_A$, ω, and q' as a function of T or x.

It is therefore mathematically convenient to transform $T \to \theta$, where $\theta = T - T^\circ_s$ in Eq. (9), yielding

$$\dot{m}_A \frac{d\theta}{dx} \left(c_p + \frac{h^\circ_{fg}}{\theta} \right) = q' \tag{10}$$

where we have also made the substitution $1/\theta = 1/\omega \times d\omega/d\theta$ based on the linearization of the BPE curve. In reaching Eq. (10), we have also neglected the $\omega(\partial h_B/\partial\omega)$ term in Eq. (9), which is related to the differential heat of dilution. For typical aqueous solutions, this term is much less than the latent heat term[1]. From solute conservation,

$$\dot{m}_A(T) = \frac{\dot{m}_{A0}\omega_0}{\omega(T)} = \frac{\dot{m}_{A0}\theta_0}{\theta} \tag{11}$$

where the subscript 0 denotes the inlet state, i.e., at $x = 0$. The heat transfer rate per unit length can be written as $q' = U_x \mathscr{P}(\theta_H - \theta)$, where U_x is the relevant, local overall heat transfer coefficient, and $\mathscr{P} = A/L$ is the appropriate perimeter, or heat transfer area A per unit length L, and $\theta_H = T_H - T^\circ_s$ corresponds to the bulk temperature of the isothermal stream driving the evaporation. With these substitutions and some algebra, Eq. (10) can be written in an integrable form:

$$\dot{m}_{A0} c_p \theta_0 \int_0^{\theta(x/L)} \left[\frac{1 + h^\circ_{fg}/c_p\theta}{\theta(\theta_H - \theta)} \right] d\theta = \int_0^{x/L} U_x A \, d\left(\frac{x}{L}\right) \tag{12}$$

where the right hand side integrates to the average overall heat conductance between 0 and x/L, $(\overline{UA})_{0\to x/L}$.

Integration of Eq. (12) gives an implicit equation for the temperature distribution within the heat exchanger:

$$\frac{(\overline{UA})_{0\to x/L}}{\dot{m}_{A0}c_p}\left(\frac{x}{L}\right) = \gamma \ln\left(\frac{1-\gamma^{-1}}{1-\gamma^{-1}\theta_0/\theta}\right)\left(1 + \frac{1}{\mathrm{Ja}_H}\right) + \frac{1}{\mathrm{Ja}_H}\left(1 - \frac{\theta_0}{\theta}\right) \tag{13}$$

where we have introduced the following dimensionless parameters:

$$\gamma = \theta_0/\theta_H \tag{14}$$

$$\mathrm{Ja}_H = c_p\theta_H/h^\circ_{fg} \tag{15}$$

3.1 Effectiveness

Effectiveness is defined as

$$\varepsilon = \frac{T_L - T_0}{T_H - T_0} = \frac{\theta_L/\theta_0 - 1}{\gamma^{-1} - 1} \tag{16}$$

where the subscript L denotes the outlet of the evaporator. At 100% effectiveness, the concentrate stream outlet is in thermal equilibrium with the isothermal stream driving the evaporation at T_H. Consequently, because of the linearization of the BPE curve, $1/\gamma$ is approximately equivalent to the maximum solute concentration divided by the inlet concentration, i.e., the concentration factor at 100% effectiveness:

$$\mathrm{CF}_{\max} = \frac{w_H}{w_0} \approx \frac{\theta_H}{\theta_0} = 1/\gamma \tag{17}$$

where w is the mass fraction of solutes.

As $x/L \to 1$, Eq. (13) can be rewritten to yield the desired effectiveness-NTU relationship:

$$\mathrm{NTU} = \gamma \ln\left[1 - \frac{\varepsilon}{\gamma(\varepsilon - 1)}\right]\left(1 + \frac{1}{\mathrm{Ja}_H}\right) + \frac{1}{\mathrm{Ja}_H}\left[1 - \frac{1}{1 + \varepsilon(1/\gamma - 1)}\right] \tag{18}$$

[1] The term $\omega(\partial h_B/\partial\omega) = -h_{\mathrm{dil}}/\omega$, where h_{dil} is the differential enthalpy of dilution. Based on enthalpy data from [33], for a 3 mol/kg NaCl solution at 60° C, $\omega(\partial h_B/\partial\omega) \approx 0.44$ kJ/kg$_\mathrm{A}$ – about five orders of magnitude less than h°_{fg}/ω.

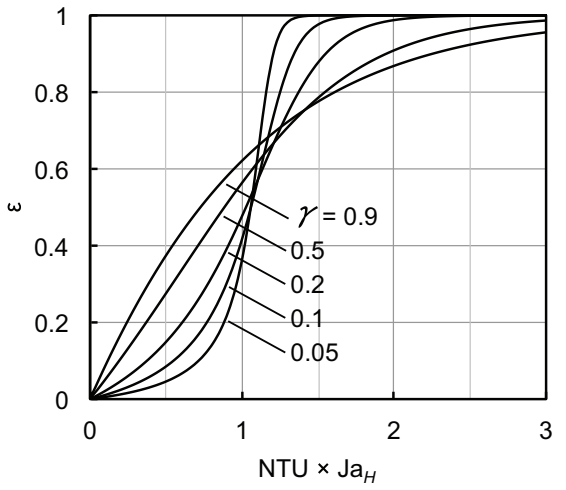

Fig. 3: Effectiveness-NTU curves for saline evaporators: at low max recoveries (as γ approaches one), the evaporator behaves like a single stream heat exchanger; at lower γ the temperature distribution is more nonlinear.

where

$$\mathrm{NTU} = \frac{\overline{UA}}{\dot{m}_{A0} c_p} \tag{19}$$

and $\overline{UA}$ is the average overall heat conductance. When A is not a function of x, e.g., in the case of a flat plate, $\overline{UA} = \overline{U}A$, where $\overline{U}$ is the average overall heat transfer coefficient, i.e., $\int_0^1 U_x \, d(x/L)$. When $\mathrm{Ja}_H \ll 1$, as is typical for evaporating aqueous solutions, the independent parameters NTU and Ja_H collapse onto a single parameter, $\mathrm{NTU} \times \mathrm{Ja}_H$, as can be seen readily from examination of Eq. (18).

Solutions to Eq. (18), plotted as effectiveness vs. $\mathrm{NTU} \times \mathrm{Ja}_H$ are shown in Fig. 3. At lower γ (higher $\mathrm{CF}_{\max}$), the temperature profile becomes more nonlinear as more evaporation has a greater effect on the effective heat capacity of the evaporating stream.

3.2 Evaporated Fraction

An additional parameter of importance in the analysis of evaporators is the evaporated fraction, which we denote χ. The evaporated fraction χ is defined as the mass flow rate of vapor per unit feed solution:

$$\chi = \frac{\dot{m}_v}{(1+\omega_0)\dot{m}_{A0}} \tag{20}$$

Because of the relationship between saturation temperature and solute concentration, χ can be written as a function of ε. From solute mass conservation $\dot{m}_{AL} = \omega_0 \dot{m}_{A0}/\omega_L$; from overall mass conservation, $\dot{m}_v = (1+\omega_0)\dot{m}_{A0} - (1+\omega_L)\dot{m}_{AL}$. Thus, the evaporated fraction can be written as a function of solute concentrations as

$$\chi = 1 - \left(\frac{\omega_0}{1+\omega_0}\right)\left(\frac{1+\omega_L}{\omega_L}\right) = 1 - \frac{w_0}{w_L} \tag{21}$$

The maximum evaporated fraction, $\chi_{\max}$, occurs when the evaporating stream is in thermal equilibrium with the heat source at T_H, or where the solute concentration at $x/L = 1$ is equal to ω_H. Thus, the definition of $\chi_{\max}$ is readily written by replacing ω_L with ω_H in Eq. (21). By the linear BPE relationship, we substitute ω_L/ω_0 and ω_0/ω_H for θ_L/θ_0 and γ in Eq. (16), and solve for $\chi/\chi_{\max}$ using the definitions above to find

$$\frac{\chi}{\chi_{\max}} = \frac{\varepsilon}{1+(\varepsilon-1)(1+\omega_0)\chi_{\max}} \tag{22}$$

4 Perturbation Analysis for Small Concentration Factors

For small concentration factors, we expect single stream heat exchanger like behavior, as neither evaporative mass loss nor boiling point elevation have significant effects on the effective heat capacity rate of the evaporating stream. A perturbation analysis around $\gamma = 1$ reveals such behavior, confirming that the model behaves as expected.

Let $\mu \equiv 1-\gamma$. Rewriting Eq. (18) in terms of μ, we find

$$\begin{aligned}\mathrm{NTU} \times \mathrm{Ja}_H = (1-\mu)\ln\left[1 - \frac{\varepsilon}{(1-\mu)(\varepsilon-1)}\right](1+\mathrm{Ja}_H) \\ + \left[1 - \frac{1}{1+\varepsilon\left(\frac{\mu}{1-\mu}\right)}\right]\end{aligned} \tag{23}$$

Expanding Eq. (23) in terms of μ yields

$$\begin{aligned}\mathrm{NTU} \times \mathrm{Ja}_H = -(1+\mathrm{Ja}_H)\ln(1-\varepsilon) \\ + \left\{(1+\mathrm{Ja}_H)\Big[\varepsilon + \ln(1-\varepsilon)\Big] + \varepsilon\right\}\mu \\ + \mathscr{O}(\mu^2) + \ldots\end{aligned} \tag{24}$$

Then, for small μ, we can neglect the higher order terms and the ε–NTU relationship can be expressed as

$$\frac{\mathrm{NTU} \times \mathrm{Ja}_H - \varepsilon\mu}{1+\mathrm{Ja}_H} - \varepsilon\mu = -(1-\mu)\ln(1-\varepsilon) \tag{25}$$

We consider two further simplifications of this of this equation: (1) the case where $\mathrm{Ja}_H \ll 1$, as is typical for aqueous solutions; and (2) the case where $\mathrm{Ja}_H \to \infty$, which corresponds to no latent heat effects [cf. Eq. (10)]. In the first case, Eq. (25) reduces to

$$\varepsilon = 1 - \exp\left[-\frac{\mathrm{NTU} \times \mathrm{Ja}_H - 2\mu\varepsilon}{1-\mu}\right] \tag{26}$$

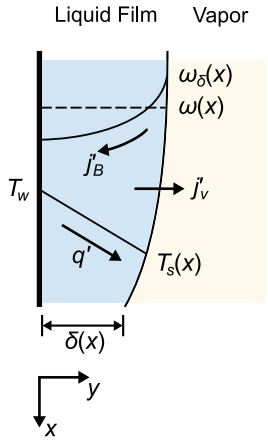

Fig. 4: A schematic of the mass diffusion and heat transfer processes occurring in the film: a temperature difference $\big(T_w - T_s(x)\big)$ drives solvent evaporation j'_v at the vapor–liquid interface, increasing the local (non-volatile) solute concentration ω_δ and driving a diffusive flux of solute j'_B back towards the film bulk.

By the *ansatz* of our perturbation analysis, $\mu \ll 1$; NTU $\times$ Ja_H is $\mathscr{O}(1)$ (see Fig. 3), and $0 < \varepsilon < 1$. Consequently, the argument of the exponential is very nearly $-\mathrm{NTU} \times \mathrm{Ja}_H$, and Eq. (26) behaves like the effectiveness–NTU relationship for a single stream heat exchanger in $\mathrm{NTU} \times \mathrm{Ja}_H$, i.e., $\varepsilon = 1 - \exp(-\mathrm{NTU} \times \mathrm{Ja}_H)$. This behavior can be seen in Fig. 3 for values of γ that approach unity.

In the second case, Eq. (25) reduces to:

$$\varepsilon = 1 - \exp\left[-\frac{\mathrm{NTU} - \mu\varepsilon}{1-\mu}\right] \tag{27}$$

Again, because $\mu \ll 1$, we again see the expected limiting behavior, i.e., that of a single stream heat exchanger.

5 Calculation of the Film Heat Transfer Coefficient

Because classical expressions for the film heat transfer coefficients are only valid for constant temperature differences across the film, we derive new relationships that account for the varying ΔT across the film owing to boiling point elevation. To do so, we solve the coupled heat, mass, and momentum problem. Two cases are considered: (1) a film with arbitrary laminar or wavy-laminar hydrodynamics in the limiting case of no solute mass transfer and (2) a laminar film with non-zero solute mass transfer. In both cases, we assume no nucleate boiling occurs. The heat and mass transfer processes in the film are illustrated in Fig. 4.

5.1 Laminar or Wavy-Laminar Film without Mass Transfer

Neglecting the much smaller sensible heat terms in the film energy balance (cf. Eq. (6)), a simplified equation representing energy conservation on the differential control volume in Fig. 2 shows that the latent heat associated with evaporation is conducted through the film:

$$-h_{fg}\frac{d\Gamma}{dx} = \frac{k}{\delta}\left(\Delta T^\circ - K_b\omega_\delta\right) \tag{28}$$

where Γ is the local mass flow rate of the film per unit plate width, δ is the local film thickness, $\Delta T^\circ = T_w - T_s^\circ$, and ω_δ is the solute concentration at the vapor–liquid interface, and k/δ is the local heat transfer coefficient, reflecting the usual linear temperature profile approximation in laminar falling film analysis [25,26] (see Fig. 4). The term $K_b\omega_\delta$ is the local BPE, which varies with the downstream distance x.

For the limiting case of no solute diffusion, which is a reasonable approximation for salt water (see Sec. 2.2), we approximate $\omega_\delta = \omega$, the average concentration across the film. By solute conservation, $w_0\Gamma_0 = w\Gamma$, which, by the conversion $w = \omega/(1+\omega)$ can be expressed in mass ratio terms as

$$\omega = \frac{w_0\Gamma_0}{\Gamma - w_0\Gamma_0} \tag{29}$$

Substituting Eqs. (29) into Eq. (28) yields

$$\frac{d\Gamma}{dx} = -\frac{k}{\delta h_{fg}}\left(\Delta T^\circ - \frac{K_b w_0\Gamma_0}{\Gamma - w_0\Gamma_0}\right) \tag{30}$$

The average heat transfer coefficient is defined in the usual manner as

$$\bar{h}_{\mathrm{conv}} = \frac{1}{L}\int_0^L \frac{k}{\delta}\,dx \tag{31}$$

where the integrand is the local heat transfer coefficient, $h_{\mathrm{conv}} = k/\delta$. Transforming the variable of integration from x to Γ, we find

$$\bar{h}_{\mathrm{conv}} = \frac{k}{L}\int_{\Gamma_0}^{\Gamma_L} \frac{1}{\delta}\left(\frac{dx}{d\Gamma}\right) d\Gamma \tag{32}$$

Substituting Eq. (30) into Eq. (32), the local film thickness δ cancels, and the resulting average heat transfer coefficient is thus independent of film hydrodynamics. Carrying out the integration yields

$$\bar{h}_{\mathrm{conv}} = \frac{h_{fg}}{\Delta T^\circ L}\Bigg[\Gamma_0 - \Gamma_L + w_0\Gamma_0\frac{K_b}{\Delta T^\circ}\ln\left(\frac{\frac{1}{w_0} - \frac{K_b}{\Delta T^\circ} - 1}{\frac{\Gamma_L}{w_0\Gamma_0} - \frac{K_b}{\Delta T^\circ} - 1}\right)\Bigg] \tag{33}$$

Recasting Eq. (33) in dimensionless form, the average Nusselt number as a function of the film Reynolds number,

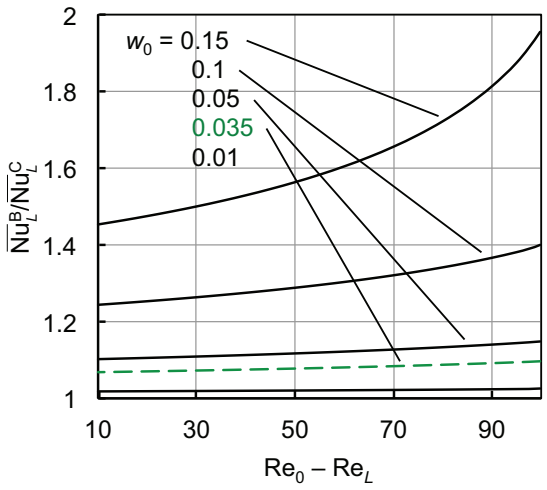

Fig. 5: Ratio of Nu with BPE effects and zero mass transfer resistance [Eq. (34)] to the classical Nusselt solution for an NaCl-like solution with $\Delta T^\circ = 10$ K, $h_{fg}\mu/4k = 7.42 \cdot 10^5$, and $K_b = 17.1$ K: the BPE effects are more pronounced at higher inlet concentrations and higher concentration factors, or higher $\mathrm{Re}_0 - \mathrm{Re}_L$. The dashed green line, $w_0 = 0.035$, represents seawater salinity.

$\mathrm{Re} = 4\Gamma/\mu$, the Prandtl number, $\mathrm{Pr} = \mu c_p/k$, and the Jakob number, $\mathrm{Ja}^\circ = c_p\Delta T^\circ/h_{fg}$, is

$$\overline{\mathrm{Nu}}_L^B = \frac{\mathrm{Pr}}{4\,\mathrm{Ja}^\circ}\left[\mathrm{Re}_0 - \mathrm{Re}_L + w_0\mathrm{Re}_0\frac{K_b}{\Delta T^\circ}\ln\left(\frac{\frac{1}{w_0} - \frac{K_b}{\Delta T^\circ} - 1}{\frac{\mathrm{Re}_L}{w_0\mathrm{Re}_0} - \frac{K_b}{\Delta T^\circ} - 1}\right)\right] \tag{34}$$

which limits correctly to the expression from Nusselt theory, $\overline{\mathrm{Nu}}_L^C = \mathrm{Pr}(\mathrm{Re}_0 - \mathrm{Re}_L)/4\,\mathrm{Ja}^\circ$, when $K_b = 0$ and boiling point elevation effects go to zero. Eqs. (33) and (34) are valid for laminar and wavy-laminar films ($\mathrm{Re} < 5800\,\mathrm{Pr}^{-1.06}$ [25]) so long as the solute mass transfer resistance is small, i.e., Eq. (2) is near unity.

Fig. 5 shows the ratio of Nu with BPE effects and zero mass transfer [Eq. (34)] to the classical solution, $\overline{\mathrm{Nu}}_L^C$. As the inlet concentration and concentration factor increase, the effects of BPE become more pronounced.

5.2 Laminar Film with Mass Transfer

When solute diffusion across the film must be considered, an integral method analysis of the mass transfer boundary layer (shown schmatically in Fig. 4) coupled with Eq. (28) yields an expression for the average heat transfer coefficient. For a fully-developed mass transfer boundary layer, Chun and Seban [27] used the integral method assuming a parabolic form of $w = f(\delta - y)$ to show

$$\frac{w_\delta}{w_0} = \frac{\Gamma_0}{\Gamma}\left(1 + \frac{\delta}{5\rho\mathscr{D}}\frac{d\Gamma}{dx}\right)^{-1} \tag{35}$$

where $\mathscr{D}$ is the diffusivity of the solute in the mixture and ρ is the mixture density. We neglect the entrance length, as it is typically only relevant for small concentration factors [27]. From classical Nusselt theory [3,25,26], momentum conservation on a laminar film ($\mathrm{Re} < 30$ [25]) relates its thickness to its flow rate:

$$\delta = \left(\frac{3\mu\Gamma}{\rho(\rho - \rho_v)g}\right)^{\frac{1}{3}} = D_0\Gamma^{\frac{1}{3}} \tag{36}$$

where the prefactor on $\Gamma^{\frac{1}{3}}$ has been defined as D_0 for convenience. With the aid of Eq. (36) and the relationship $w = \omega/(1+\omega)$, we can rewrite Eq. (35) in terms of the solute mass ratio and the film flow rate:

$$\omega_\delta = \frac{w_0\Gamma_0}{\Gamma + \frac{D_0}{5\rho\mathscr{D}}\Gamma^{\frac{4}{3}}\frac{d\Gamma}{dx} - w_0\Gamma_0} \tag{37}$$

Substituting Eq. (36) and Eq. (37) into the film energy balance, Eq. (28), we find

$$\frac{d\Gamma}{dx} = -\frac{k}{D_0 h_{fg}\Gamma^{\frac{1}{3}}}\left[\Delta T^\circ - \frac{K_b w_0\Gamma_0}{\Gamma + \frac{D_0}{5\rho\mathscr{D}}\Gamma^{\frac{4}{3}}\frac{d\Gamma}{dx} - w_0\Gamma_0}\right] \tag{38}$$

With some algebra, Eq. (38) can be rewritten as a quadratic equation in $d\Gamma/dx$:

$$\left(\frac{d\Gamma}{dx}\right)^2 C_0 + \frac{d\Gamma}{dx}\Gamma^{-1/3}\left(C_1 - \frac{C_2}{\Gamma}\right) + \Gamma^{-2/3}\left(C_3 - \frac{C_4}{\Gamma}\right) = 0 \tag{39}$$

where we have made the following substitutions for ease of reading:

$$C_0 = \frac{D_0}{5\rho\mathscr{D}} \tag{40}$$

$$C_1 = 1 + \frac{k\Delta T^\circ}{5\rho\mathscr{D}h_{fg}} \tag{41}$$

$$C_2 = w_0\Gamma_0 \tag{42}$$

$$C_3 = \frac{\Delta T^\circ k}{D_0 h_{fg}} \tag{43}$$

$$C_4 = \frac{w_0\Gamma_0(\Delta T_s^\circ + K_b)k}{D_0 h_{fg}} \tag{44}$$

By the quadratic formula, Eq. (39) can be solved for $d\Gamma/dx$

$$\frac{d\Gamma}{dx} = \frac{1}{2C_0\Gamma^{1/3}}\left[\left(\frac{C_2}{\Gamma} - C_1\right) + \sqrt{\left(C_1 - \frac{C_2}{\Gamma}\right)^2 - 4C_0\left(C_3 - \frac{C_4}{\Gamma}\right)}\right] \tag{45}$$

where we have chosen the positive root so that Eq. (45) limits correctly to the classical Nusselt expression, $d\Gamma/dx = -k\Delta T^\circ/\delta h_{fg}$, when BPE and the mass transfer resistance go to zero; i.e., when $K_b \to 0$ and $\mathscr{D} \to \infty$, respectively (details in App. B).

As with the analysis in Sec. 5.1, the average heat transfer coefficient can be expressed as an integral over the film flow rate Γ by Eq. (32). Substituting in Eqs. (45) and (36) into our definition of $\bar{h}_{\text{conv}}$, Eq. (32), we obtain an integral expression for the average heat transfer coefficient:

$$\bar{h}_{\text{conv}} = \frac{2k}{L}\int_{\Gamma_0}^{\Gamma_L}\left[\left(\frac{C_2}{\Gamma} - C_1\right) + \sqrt{\left(C_1 - \frac{C_2}{\Gamma}\right)^2 - 4C_0\left(C_3 - \frac{C_4}{\Gamma}\right)}\right]^{-1} d\Gamma \quad \times 1/(5\rho D) \tag{46}$$

which has the solution, in dimensionless number form,

$$\overline{\text{Nu}}_L^{\text{MB}} = \frac{\bar{h}_{\text{conv}}L}{k} = B_0\left\{B_1 \ln\left(\frac{F_1(\Gamma_0)}{F_1(\Gamma_L)}\right) - B_2\left[B_3\left(F_2(\Gamma_0) - F_2(\Gamma_L)\right) + B_4 \ln\left(\frac{F_3(\Gamma_0)}{F_3(\Gamma_L)}\right)\right]\right\} \quad \times 1/(5\rho D) \tag{47}$$

Expressions for the constants B_i and the functions F_i are given in Appendix A. Eq. (47) is valid for laminar films ($\text{Re} < 30$) with fully-developed mass transfer boundary layers.

Fig. 6 shows the ratio of Nu with BPE effects and nonzero mass transfer, $\overline{\text{Nu}}_L^{\text{MB}}$, to the classical solution, $\overline{\text{Nu}}_L^{\text{C}}$. Like Fig. 5, as the inlet concentration and concentration factor increase, the effects of BPE become more pronounced. However, the effects are modulated by the mass transfer modeling, which accounts for the difference between the solute concentration in the bulk and at the vapor–liquid interface.

6 Conclusions

An analytical effectiveness–NTU relationship was developed for evaporators with linear, non-negligible increases in boiling point elevation. A perturbation analysis revealed that the model behaves as expected for limiting cases. Analytical expressions for evaluating the heat transfer coefficient

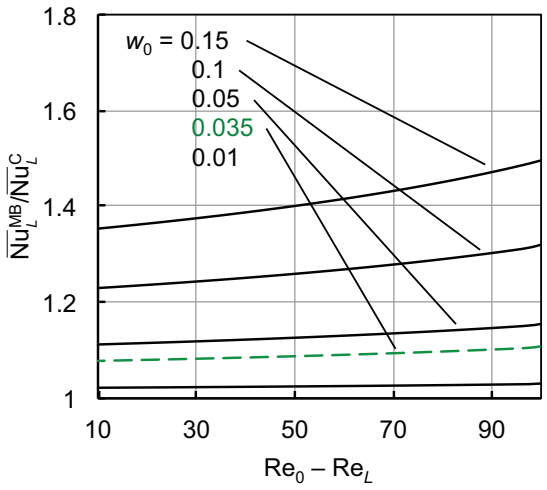

Fig. 6: Ratio of Nu with BPE effects and finite mass transfer resistance [Eq. (47)] to the classical Nusselt solution for an NaCl-like solution with $\Delta T^\circ = 10$ K, $h_{fg}\mu/4k =$ 742 , $K_b = 17.1$ K, and $\mathscr{D} = 2\times10^{-9}$ m/s: the BPE effects are again more pronounced at higher solute feed concentrations and higher concentration factors, or higher $\text{Re}_0 - \text{Re}_L$. The dashed green line, $w_0 = 0.035$, represents seawater salinity.

in evaporators with linear, non-negligible increases in boiling point elevation were also developed. The model can be applied in a variety of process engineering applications to size and rate evaporators.

Acknowledgements

The authors would like to thank the King Fahd University of Petroleum and Minerals for funding the research reported in this paper through the Center for Clean Water and Clean Energy at MIT and KFUPM under project number R13-CW-10. GPT would like to thank Wilko Rohlfs for the insightful discussions that greatly improved this work. Finally, the authors gratefully acknowledge the helpful comments of two anonymous reviewers.

References

[1] Standiford, F. C., 2000. "Evaporation". In *Kirk-Othmer Encyclopedia of Chemical Technology*. John Wiley & Sons.

[2] Glover, W. B., 2004. "Selecting evaporators for process applications". *Chemical Engineering Progress*, December, pp. 26–33.

[3] Nußelt, W., 1916. "Die Oberflächenkondensation des Wasserdampfes". *Zeitschrift des Vereins Deutscher Ingenieure,* **60**, pp. 541–546.

[4] Chen, M. M., 1961. "An Analytical Study of Laminar Film Condensation: Part 1—Flat Plates". *Journal of Heat Transfer,* **83**(1), February, pp. 48–54.

[5] Chun, K. R., and Seban, R. A., 1971. "Heat transfer

to evaporating liquid films". *Journal of Heat Transfer,* **93**(4), November, pp. 391–396.

[6] Brumfield, L. K., and Theofanous, T. G., 1976. "On the prediction of heat transfer across turbulent liquid films". *Journal of Heat Transfer,* **98**(3), pp. 496–502.

[7] Mudawwar, I. A., and El-Masri, M. A., 1986. "Momentum and heat transfer across freely-falling turbulent liquid films". *International Journal of Multiphase Flow,* **12**(5), pp. 771–790.

[8] Shmerler, J. A., and Mudawwar, I., 1988. "Local evaporative heat transfer coefficient in turbulent free-falling liquid films". *International Journal of Heat and Mass Transfer,* **31**(4), pp. 731–742.

[9] Marsh, W. J., and Mudawar, I., 1989. "Predicting the onset of nucleate boiling in wavy free-falling turbulent liquid films". *International Journal of Heat and Mass Transfer,* **32**(2), pp. 361–378.

[10] Parken, W. H., Fletcher, L. S., Sernas, V., and Han, J. C., 1990. "Heat transfer through falling film evaporation and boiling on horizontal tubes". *Journal of Heat Transfer,* **112**(3), pp. 744–750.

[11] Ueda, T., Inoue, M., and Nagatome, S., 1981. "Critical heat flux and droplet entrainment rate in boiling of falling liquid films". *International Journal of Heat and Mass Transfer,* **24**(7), pp. 1257–1266.

[12] Fletcher, L. S., Sernas, V., and Galowin, L. S., 1974. "Evaporation from thin water films on horizontal tubes". *Industrial & Engineering Chemistry Process Design and Development,* **13**(3), pp. 265–269.

[13] Yung, D., Lorenz, J. J., and Ganic, E. N., 1980. "Vapor/liquid interaction and entrainment in falling film evaporators". *Journal of Heat Transfer,* **102**, pp. 20–25.

[14] Chyu, M. C., and Bergles, A. E., 1987. "An analytical and experimental study of falling-film evaporation on a horizontal tube". *Journal of Heat Transfer,* **109**, pp. 983–990.

[15] Kocamustafaogullari, G., and Chen, I. Y., 1988. "Falling film heat transfer analysis on a bank of horizontal tube evaporator". *AIChE Journal,* **34**(9), pp. 1539–1549.

[16] Han, J.-C., and Fletcher, L. S., 1985. "Falling film evaporation and boiling in circumferential and axial grooves on horizontal tubes". *Industrial & Engineering Chemistry Process Design and Development,* **24**(3), pp. 570–575.

[17] Roques, J. F., Dupont, V., and Thome, J. R., 2002. "Falling film transitions on plain and enhanced tubes". *Journal of Heat Transfer,* **124**, pp. 491–499.

[18] Li, W., Wu, X.-Y., Luo, Z., and Webb, R. L., 2011. "Falling water film evaporation on newly-designed enhanced tube bundles". *International Journal of Heat and Mass Transfer,* **54**, pp. 2990–2997.

[19] Rose, J. W., 1998. "Condensation heat transfer fundamentals". *Chemical Engineering Research and Design,* **76**(2), pp. 143–152.

[20] Thome, J. R., 1999. "Falling film evaporation: state-of-the-art review of recent work". *Journal of Enhanced Heat Transfer,* **6**, pp. 263–278.

[21] Ribatski, G., and Jacobi, A. M., 2005. "Falling-film evaporation on horizontal tubes—a critical review". *International Journal of Refrigeration,* **28**, pp. 635–653.

[22] Mistry, K., Antar, M. A., and Lienhard V, J. H., 2013. "An improved model for multiple effect distillation". *Desalination and Water Treatment,* **51**, pp. 807–821.

[23] Thiel, G. P., Tow, E. W., Banchik, L. D., Chung, H., and Lienhard V, J. H., 2015. "Energy consumption in desalinating produced water from shale oil and gas extraction". *Desalination,* **366**, pp. 94–112.

[24] Kays, W. M., and London, A. L., 1998. *Compact Heat Exchangers*, 3rd ed. Krieger.

[25] Mills, A. F., 1998. *Heat Transfer*, 2nd ed. Prentice Hall.

[26] Lienhard IV, J. H., and Lienhard V, J. H., 2011. *A Heat Transfer Textbook*, 4th ed. Phlogiston Press.

[27] Chun, K. R., and Seban, R. A., 1972. "Performance prediction of falling-film evaporators". *Journal of Heat Transfer*, November, pp. 432–436.

[28] Fletcher, L. S., Sernas, V., and Parken, W. H., 1975. "Evaporation heat transfer coefficients for thin sea water films on horizontal tubes". *Industrial & Engineering Chemistry Process Design and Development,* **14**, pp. 411–416.

[29] Glasstone, S., 1947. *Thermodynamics for Chemists*. D. Van Nostrand Company.

[30] Saxton, B., Austin, J. B., Dietrich, H. G., Fenwick, F., Fleischer, A., Frear, G. L., Roberts, E. J., Smith, R. P., Solomon, M., and Spurlin, H. M., 1928. "Boiling-point elevations, non-volatile solutes". In *International critical tables of numerical data, physics, chemistry and technology*, E. W. Washburn, ed., Vol. III. McGraw-Hill, pp. 324–350.

[31] Scatchard, G., Hamer, W. J., and Wood, S. E., 1938. "Isotonic solutions. i. the chemical potential of water in aqueous solutions of sodium chloride, potassium chloride, sulfuric acid, sucrose, urea and glycerol at 25°.". *Isotonic Solutions,* **60**, pp. 3061–3070.

[32] Brown, E. H., and Whitt, C. D., 1952. "Vapor pressure of phosphoric acids". *Industrial and Engineering Chemistry,* **44**(3), pp. 615–618.

[33] Messikomer, E. E., and Wood, R. H., 1975. "The enthalpy of dilution of aqueous sodium chloride at 298.15 to 373.15 k, measured with a flow calorimeter". *Journal of Chemical Thermodynamics,* **7**, pp. 119–130.

A Constants in the Laminar Film Heat Transfer Coefficient

The constants B_i in Eq. (47) are:

$$B_0 = -\left(2C_0C_3^2B_2\right)^{-1} \tag{48}$$

$$B_1 = C_1C_2C_3 - C_1^2C_4 + 2C_0C_3C_4 \tag{49}$$

$$B_2 = \sqrt{C_1^2 - 4C_0C_3} \tag{50}$$

$$B_3 = C_3 \tag{51}$$

$$B_4 = C_1C_4 - C_2C_3 \tag{52}$$

$$\tag{53}$$

The functions F_i in Eq. (47) are:

$$F_1(x) = 2C_0C_4 - C_1C_2 + xB_2\left(B_2 + \sqrt{G(x)}\right) \tag{54}$$

$$F_2(x) = x\left(C_1 + \sqrt{G(x)}\right) \tag{55}$$

$$F_3(x) = C_2^2C_3 + C_2\left[C_3x\sqrt{G(x)} - C_1(C_4 + C_3x)\right] + C_4\left[2C_0(C_4 - C_3x) + C_1x\left(C_1 - \sqrt{G(x)}\right)\right] \tag{56}$$

where

$$G(x) = \frac{C_2^2 - 2C_1C_2x + x\left(4C_0C_4 + B_2^2x\right)}{x^2} \tag{57}$$

B Zero Mass Transfer Limit

The limit $\mathscr{D} \to \infty$ in Eq. (45) corresponds to no mass transfer resistance. The limit is indeterminate $(0/0)$, so we apply L'Hopital's Rule, differentiating the numerator and denominator with respect to $\mathscr{D}$:

$$\lim_{\mathscr{D}\to\infty}\frac{d\Gamma}{dx} = \lim_{\mathscr{D}\to\infty}\frac{\frac{d}{d\mathscr{D}}\left[\left(\frac{C_2}{\Gamma} - C_1\right) + \sqrt{\left(C_1 - \frac{C_2}{\Gamma}\right)^2 - 4C_0\left(C_3 - \frac{C_4}{\Gamma}\right)}\right]}{\frac{d}{d\mathscr{D}}\left(2C_0\Gamma^{1/3}\right)} \tag{58}$$

Carrying out the differentiation, we find

$$\lim_{\mathscr{D}\to\infty}\frac{d\Gamma}{dx} = \lim_{\mathscr{D}\to\infty}\frac{-1}{2C_0\Gamma^{1/3}}\left\{(C_1 - 1) + \frac{1}{2}\left[\left(C_1 - \frac{C_2}{\Gamma}\right)^2 - 4C_0\left(C_3 - \frac{C_4}{\Gamma}\right)\right]^{-1/2}\left[2\left(C_1 - \frac{C_2}{\Gamma}\right)(1 - C_1) + 4C_0\left(C_3 - \frac{C_4}{\Gamma}\right)\right]\right\} \tag{59}$$

which, upon taking the limit, reduces to

$$\lim_{\mathscr{D}\to\infty}\frac{d\Gamma}{dx} = -\frac{\left(C_3 - \frac{C_4}{\Gamma}\right)}{\Gamma^{1/3}\left(1 - \frac{C_2}{\Gamma}\right)} \tag{60}$$

Substituting in for C_2, C_3, and C_4, Eq. (60) becomes

$$\lim_{\mathscr{D}\to\infty}\frac{d\Gamma}{dx} = -\frac{k\Delta T^\circ}{D_0h_{fg}\Gamma^{1/3}}\left(1 - \frac{w_0\Gamma_0K_b/\Delta T^\circ}{\Gamma - w_0\Gamma_0}\right) \tag{61}$$

which is identical to Eq. (30), the film energy balance with no mass transfer resistance. As expected, Eq. (61) limits to the classical Nusselt expression when $K_b \to 0$ and boiling point elevation effects go to zero.